

Reaction $^{52}\text{Cr}(p,\gamma)^{53}\text{Mn}$ from 1.38 to 1.66 MeV

I. A. Al-Agil, G. U. Din, A. M. A. Al-Soraya, and S. A. Bagazi
Van de Graaff Laboratory, King Saud University, Riyadh, Saudi Arabia

J. A. Cameron

Tandem Accelerator Laboratory, McMaster University, Hamilton, Ontario, Canada L8S 4K1

(Received 12 March 1990)

The reaction $^{52}\text{Cr}(p,\gamma)^{53}\text{Mn}$ has been studied in the proton energy range 1.38–1.66 MeV ($7.91 < E_x < 8.19$ MeV). Spectra and γ -ray angular distributions at 16 of the 33 resonances provide J^π assignments and γ decay schemes for these and many of the bound states. Eight fragments of the isobaric analog of the $^{53}\text{C } \frac{5}{2}^-$ 1.006-MeV state were found near $E_x = 8.05$ MeV. Isobaric analog state centroids and widths are presented for the strong γ -decay channels and are related to the structure of the parent state.

I. INTRODUCTION

The low-lying levels of ^{53}Mn have been investigated extensively using a wide variety of reactions. High spin levels, to $\frac{27}{2}^-$, have been observed in heavy ion reactions while many low-spin states appear in $(\alpha, n\gamma)$, $(p, n\gamma)$, and (p, γ) reactions. Spin-parity assignments and decay branching from many states are summarized in Ref. 1. Higher energy levels have been located by proton stripping^{2,3} and other reactions such as (α, p) , (p, α) , and $(^7\text{Li}, ^6\text{He})$, and by resonant proton capture and scattering.

Reference 1 lists over 100 levels of ^{53}Mn up to 6 MeV, and many states, bound and unbound, are known above this. The $f_{7/2}$ shell model accounts for only six levels, of which five are below 2 MeV. The remainder arise from excitations out of the sd shell or into the fp shell. Among the latter are to be found, above 7 MeV in excitation, the analogs of ^{53}Cr levels. Early assignments were made of such analogs in ^{53}Mn of the ground and first excited levels of ^{53}Cr .²⁻⁸ In the region just above this lie a number of $l=3$ levels in ^{53}Cr . The first of these, a $\frac{5}{2}^-$ state at 1.006 MeV, has a reported analog at 8.050 MeV in ^{53}Mn with a $(^3\text{He}, d)$ spectroscopic factor of 0.78. Nearby are other $\frac{5}{2}^-$ levels of lower strength.¹⁻³ It was the objective of this investigation to study the fragmentation of this analog state in proton capture. In the course of the search for $\frac{5}{2}^-$ proton resonances in the energy range 1.38–1.66 MeV ($7.91 < E_x < 8.19$ MeV), 33 resonances were identified, of which 16 were strong enough for γ spectra and angular distributions to be obtained. Decay schemes of these resonances were developed and J^π values of a number of bound and unbound states were found. Eight $\frac{5}{2}^-$ analog state fragments are suggested between 8.0 and 8.1 MeV. Rudimentary fragmentation analysis in different decay channels is presented.

II. EXPERIMENTAL

The measurements were made at the King Saud AK and McMaster KN Van de Graaff accelerators. At both,

the beam energy spread was less than 1 keV. The targets were prepared by vacuum deposition of enriched ^{53}Cr (99.74%) to a thickness of 10–15 $\mu\text{g}/\text{cm}^2$ on tungsten backings carefully selected for low fluorine contamination. Similar attention was paid to the selection and cleaning of the tungsten beam collimating apertures.

The γ detectors used were HPGe counters with efficiencies and resolutions at 1.33 MeV of 38%, 2.0 keV and 26%, 1.7 keV, respectively. Efficiency curves and energy calibrations were made using ^{56}Co sources and the $^{27}\text{Al}(p,\gamma)^{28}\text{Si}$ reaction at the 0.992-MeV resonance. The beam energy was calibrated using the same reaction. Lines from ^{19}F and ^{27}Al contaminants, as well as room background ^{40}K , ^{137}Cs , ^{226}Ra , and ^{228}Th , provided continuous monitors of the detector energy calibration.

The yield curve was measured in steps of less than 1 keV from 1.38 to 1.66 MeV using a 10- $\mu\text{g}/\text{cm}^2$ target and the 38% detector, close to the target at 55°. The yield was obtained in the γ energy ranges 1.8–5.1, 5.1–7.4, and 7.4–8.4 MeV, respectively, taking in the capture secondary γ rays, primary transitions to high-lying levels, and those to the ground and first excited states.

In this geometry, spectra were obtained at the 16 strongest resonances for integrated beam charges of 40–100 mC and energies and intensities were found for all the primary and secondary decay branches. In forming the decay scheme for each resonance, attention was paid both to proper energy sums and to intensity balance. The branching percentages are thought to have an absolute precision of 1–2%.

Angular distributions were measured for the same 16 resonances using a 15- $\mu\text{g}/\text{cm}^2$ target and the 26% detector at 7 cm. Spectra were obtained at 0°, 30°, 45°, 60°, and 90°. A monitor Ge counter at -90° allowed compensation for small beam energy changes during long exposures (typically 10–20 mC). The angular distribution of γ rays following proton capture on a spin-zero target to a resonance of spin-parity J^π depends only on J , the final state J_f , and the γ multipolarity. The best fit distribution for each (J, J_f) combination was obtained and the reduced χ^2 plotted versus the multipole mixing ratio δ .

Since there are often a few equally acceptable solutions from such a procedure, it is useful to analyze several primary decays from each resonance. Other γ decays, too weak for angular distribution measurement, were occasionally used to select from among remaining J^π options using the assumption that only dipole and quadrupole transitions compete significantly. With the establishment of resonance spins, it was possible to study angular distributions of primary transitions to and secondary transitions from states of unknown spin.

III. RESULTS

A. Excitation functions

Figure 1 is the yield curve from the reaction $^{52}\text{Cr}(p,\gamma)^{53}\text{Mn}$ for proton energies from 1.38 to 1.66 MeV. Curve (a), for transitions to the ground and first excited states, has negligible background between resonances. Region (b) includes the 6.13-MeV γ ray from $^{19}\text{F}(p,\alpha\gamma)^{16}\text{O}$ which contributes only a low background. The strong resonances in (c) indicate considerable feeding

of highly excited states of ^{53}Mn . In all, 33 peaks are identified, most in more than one curve. The peaks are listed in Table I. The overall resolution was under 2 keV, allowing separation of doublets at 1.494/1.497, 1.522/1.526, 1.552/1.557, and 1.605/1.610 MeV. The peak positions were reproduced within 1 keV from one scan to another.

B. Resonance decay schemes

Figures 2 and 3 are examples of the γ -ray spectra, for resonances 12 and 13, at 1.494 and 1.497 MeV. The capture primary and secondary γ rays are labeled, as are the lines from target impurities and room background. The branching for 16 resonances is given in Table II. The contrast between resonances such as 12 and 13, with few and many decay branches, is evident. Of particular note in connection with the analog state search is characteristic strong branching to bound states of single particle character. One would expect an $f_{5/2}$ analog to decay preferentially to states of $f_{5/2}$ or $f_{7/2}$ character, since $M1$ decays to p states are inhibited. The ground state is

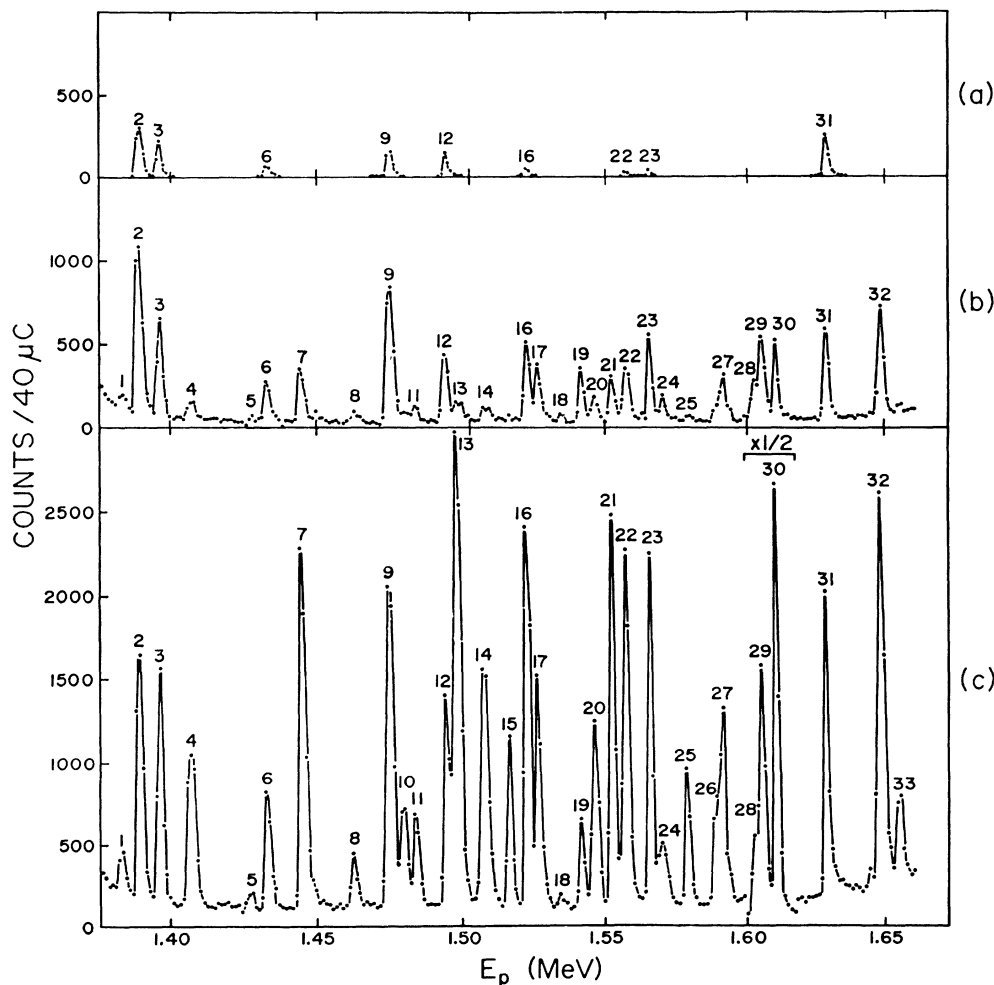


FIG. 1. Yield in the reaction $^{52}\text{Cr}(p,\gamma)^{53}\text{Mn}$ in the γ -ray energy ranges (a) 7.4–8.4 MeV, (b) 5.1–7.4 MeV, (c) 1.8–5.1 MeV.

largely $f_{7/2}$ ($C^2S=3.0$) and is fed strongly by resonances 2, 3, 9, 12, and 31. The $f_{5/2}$ strength is in the 3.129- and 3.666-MeV levels ($C^2S=0.2, 1.8$, respectively) fed by resonances 17 and 30. The $p_{3/2}$ strength is in the 1.290- and 2.407-MeV states ($C^2S=0.2, 1.5$, respectively) fed by resonances 16, 17, 29, and 32, while only resonance 30 feeds the $p_{1/2}$ 3.480-MeV state ($C^2S=0.25$).

All of the bound states populated directly from the resonances are of low spin. The low-lying high-spin states at 1.441 ($\frac{11}{2}^-$) and 1.621 ($\frac{9}{2}^-$) were populated in secondary decays. Table III summarizes the branching ratios of all

46 bound excited states populated in this work. The uncertainties range from 2 to 5%. All of the bound states had been reported previously,¹ but the 18 levels marked (a) in Table III were seen mainly in the (p, α) reaction⁹ and no previous γ decays were known.

C. Angular distributions and J^π assignments

The angular distribution results are given in Table IV and summarized in Table I. For 10 of the 16 resonances

TABLE I. Resonances in $^{52}\text{Cr}(p, \gamma)^{53}\text{Mn}$, $1.38 \leq E_p \leq 1.66$ MeV (w=weak).

Resonance No.	E_p (MeV)	E_x (MeV)	Relative intensity			Total	J^π
			E_γ : 1.8–5.1	5.1–7.4	7.4–8.4		
1	1.384	7.919	1133	469	14	1616	
2	1.390	7.925	4188	2864	717	7769	$\frac{5}{2}^-$
3	1.397	7.931	3102	1498	420	5020	$\frac{5}{2}^-$
4	1.402	7.941	3139	327	16	3482	
5	1.428	7.962	205	w	w	205	
6	1.432	7.966	1679	487	144	2310	
7	1.444	7.978	5668	738	159	6565	$\frac{3}{2}^-^a$
8	1.462	7.995	842	73	27	942	
9	1.475	8.008	4665	1898	363	6926	$\frac{5}{2}^-$
10	1.480	8.013	1362	139	31	1542	
11	1.484	8.017	1061	130	8	1199	
12	1.494	8.027	2584	739	243	3566	$\frac{5}{2}^-$
13	1.497	8.030	6525	446	37	7008	$\frac{1}{2}^-, \frac{5}{2}^-$
14	1.507	8.040	3856	208	27	4091	$\frac{3}{2}^-, \frac{5}{2}^-$
15	1.516	8.049	1565	16	9	1590	
16	1.522	8.054	4802	1002	98	5902	$\frac{5}{2}^-$
17	1.526	8.058	2875	750	31	3656	$\frac{5}{2}^-$
18	1.534	8.066	w	w	w	w	
19	1.541	8.073	830	524	86	1440	
20	1.546	8.078	2340	303	8	2651	
21	1.552	8.084	3732	395	7	4134	$\frac{5}{2}^-$
22	1.557	8.089	5113	754	63	5930	$\frac{5}{2}^-$
23	1.565	8.096	3008	686	61	3755	$\frac{3}{2}^-, \frac{5}{2}^-$, and $\frac{7}{2}^-^b$
24	1.570	8.101	302	331	19	652	
25	1.578	8.109	1495	w	w	1495	
26	1.588	8.119	3618	678	38	4334	
27	1.592	8.123	3618	678	38	4334	
28	1.603	8.134	8267	1477	35	9779	
29	1.605	8.136	8267	1477	35	9779	$\frac{3}{2}^-$
30	1.610	8.141	7513	668	19	8200	$\frac{3}{2}^-$
31	1.628	8.159	3400	871	380	4651	$\frac{5}{2}^+$
32	1.648	8.179	4480	1048	46	5574	$\frac{3}{2}^-, \frac{5}{2}^-^c$
33	1.655	8.186	1106	32	30	1168	

^aDecays to $\frac{1}{2}^+$ 2.707-MeV state.

^bDoublet.

^cParity from decay to $\frac{7}{2}^-$ 2.686-MeV state.

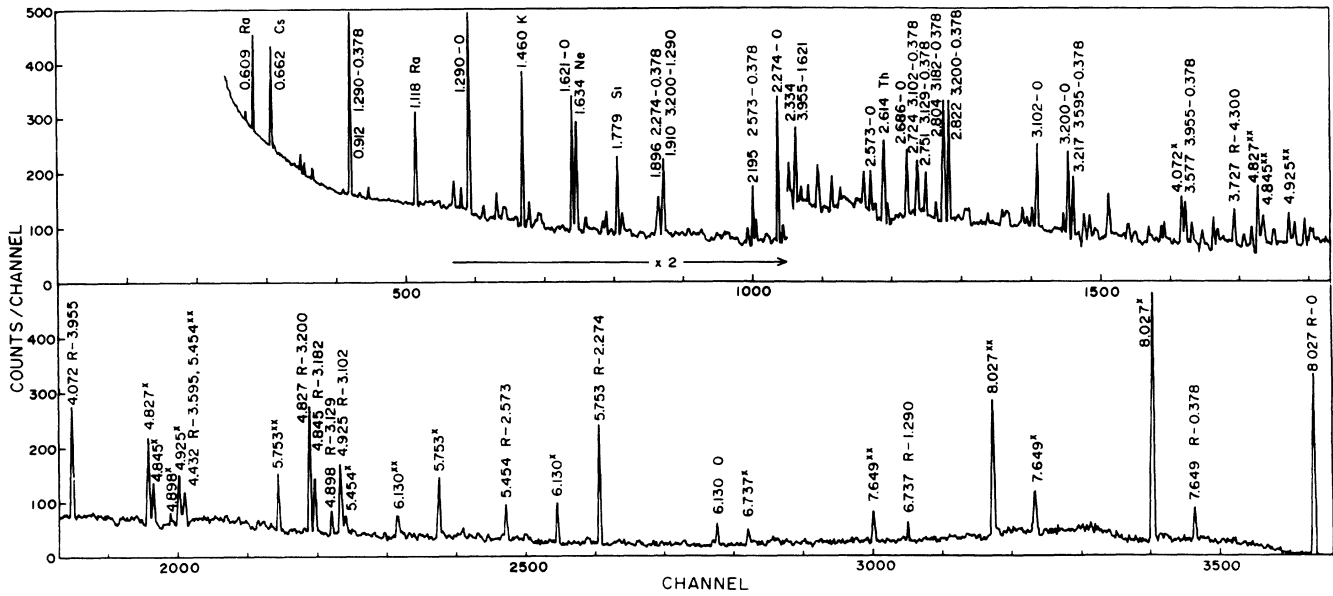


FIG. 2. Gamma-ray spectrum at resonance No. 12, $E_p = 1.494$ MeV.

measured, unique J^π assignments could be made. An example, for resonance 16, is shown in Fig. 4. In one case, the 1.494-MeV resonance No. 12, the $\frac{9}{2}^-$ ($l=5$) option was discarded as improbable. In two further cases, 7 and 31, at 1.444 and 1.628 MeV, decays to the $\frac{1}{2}^+$ 2.707-MeV level allow $\frac{5}{2}^-$ and $\frac{9}{2}^-$ possibilities to be discarded. Resonance 23 at 1.565 MeV appears to be an unresolved doublet. The $R \rightarrow 0.378$ angular distribution allows only $J^\pi = \frac{7}{2}^-$ while those for $R \rightarrow 1.290$ and $R \rightarrow 2.407$ allow $\frac{3}{2}^-$ or $\frac{5}{2}^-$ and for $R \rightarrow 2.682$, $\frac{5}{2}^-$ or $\frac{7}{2}^-$. Accordingly, a doublet must be assumed, with one spin $\frac{7}{2}^-$ and the other $\frac{3}{2}^-$ or $\frac{5}{2}^-$. No broadening is apparent either in this work,

or in the higher resonance yield curve of Vuister,⁵ so the separation of the two components is less than 1 keV.

Spins and parities of bound states can likewise be found from the γ -ray angular distributions from resonances of established J^π . As in the case of the resonances themselves, ambiguities arise and are usually resolved only if decays involving different known spins are measured. Because many of the bound states in question were fed strongly from only one resonance, secondary transitions were included in the analysis. In this way, a number of bound state assignments were made. These are given in Table V. Spins deduced from decay branching alone appear in parentheses.

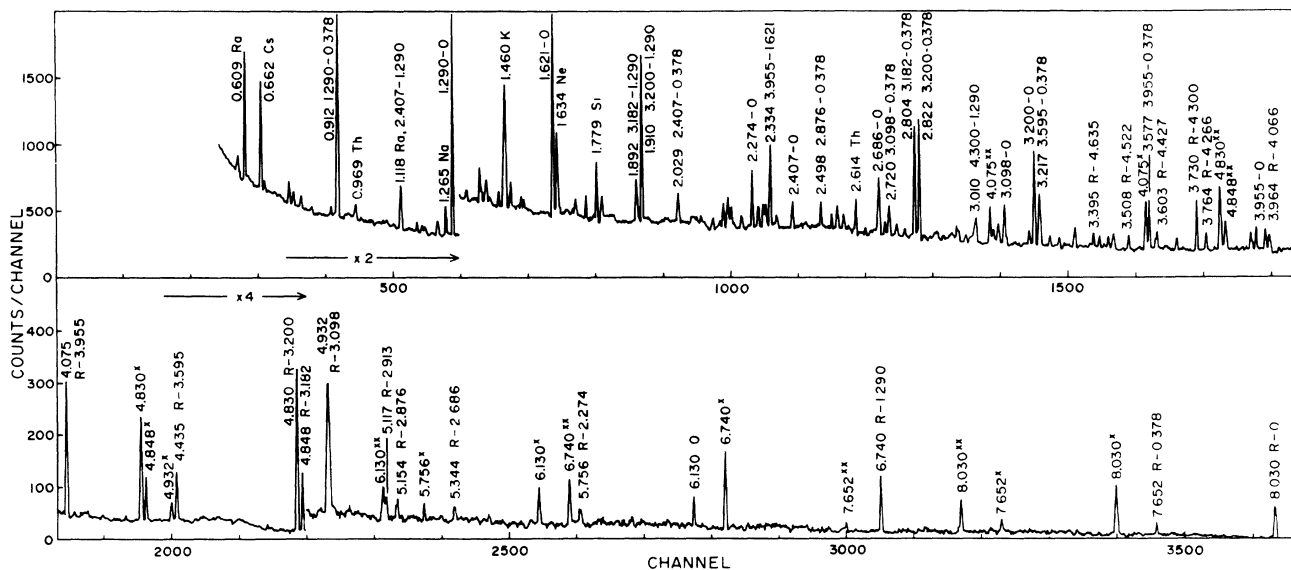


FIG. 3. Gamma-ray spectrum at resonance No. 13, $E_p = 1.497$ MeV.

IV. DISCUSSION

A. Resonance properties

The yield curve Fig. 1 agrees closely with that of Vuister,⁵ allowing for the better resolution of the latter. There is a systematic difference in the reported proton resonance energies of about 1 keV, well within the estimated systematic uncertainty in each experiment. Of

the present 33 resonances, 26 correspond directly to those of Vuister, one (No. 5) is claimed to be an impurity, and six are seen in the higher resolution of Vuister to be close doublets. These are generally dominated by one peak, with the exception of resonance No. 12 at 1.494 MeV, which consists of two approximately equal components (though no inconsistency was found in the angular distributions). In the excitation energy region 7.2–8.2 MeV, six ($^3\text{He}, d$) peaks have been reported.^{1–3} These are discussed in Sec. IV C.

TABLE II. Decay branching from $^{52}\text{Cr}(p, \gamma)^{53}\text{Mn}$ resonances.

Resonance No.	2	3	7	9	12	13	14	16	17	21	22	23	29	30	31	32
0	69	66	1	22	60	4	4	11	9	1	2	2			55	2
0.378	9		1	50	7	1	4	7	3	5	23	27	4	1	4	5
1.290	9	8	7	2	1	5	7	3	25	11	6	11	26	1	5	46
2.274	4	2	47	6	16	1		34	8	28				7		2
2.407		6	1					21	9	2		11	12	10	2	8
2.573	2				4			8	2							
2.671			4										5	24		
2.686	1	2	2	2		1	5	8	6		19	23	1	2		13
2.707			4			<1								4	1	
2.876		4	10	1		<1	12		2		14	2	3	7	3	
2.913			2	1												
3.007			2								4	2	1			2
3.098		1	4	2		8	6	3		14	8	1	6	2	12	2
3.102					2											
3.129								2	17		9	1	7	1	2	2
3.182	1			1	1	12	7		3	1	1	4	24	4		1
3.200	1				4	29	14			3		4	3			
3.381			7	6			9		1			3				
3.466		2		5								2	3		3	
3.480															9	
3.532		1														
3.595	1				1	7	5		3							
3.666							1			3	1			14		1
3.710		8													3	
3.898				1										5		
3.955	1				3	18	5	2	3			1				
3.960			1								1	1			3	
3.999											1					
4.062			3				5			10			3	5		
4.066	1			1		2									2	2
4.083			1					1					1	3	7	
4.266						2			1							4
4.300					1	7	1				3					4
4.348			1								2					
4.362												2				
4.427	1		2			1			1						1	3
4.522						1										
4.552										8	2					
4.560							10									2
4.635						1	5									
4.719										2				1		1
4.762												2				
4.780									1							
4.793									7							
4.988													4			
5.492										5						
5.998										6	2					

TABLE III. Gamma-ray branching of bound states in ^{53}Mn .

E_f	E_i	0.378	1.290	2.274	2.407	2.573	2.671	2.686	2.707	2.876	2.913	3.007	3.098	3.102	3.129	3.182	
0.0		100	62	80	43	37	60	65		15		12	17	62	10	7	
0.378			38	19	12	63	40	22		82	29	37	77	38	87	79	
1.290				1	45			13	100	3	71	51	6		3	14	
E_f	E_i	3.200	3.381 ^a	3.466 ^a	3.480	3.532	3.595	3.666	3.710 ^a	3.898	3.955 ^a	3.960 ^a	3.999 ^a	4.062	4.066	4.083 ^a	
0		33	10	58	58	18	19	87			19	48		60			
0.378		33	90	42	42	10	81	17	34	22	36	38	100	13	65	85	
1.290		32				72			16	46		17		16	23	15	
1.441		1							10								
1.621									40		31						
2.274														9			
2.407										8				2	12		
2.573																	
2.671									24								
2.686											14						
E_f	E_i	4.266	4.300 ^a	4.348	4.362 ^a	4.427	4.522 ^a	4.552 ^a	4.560 ^a	4.635 ^a	4.719 ^a	4.762 ^a	4.780	4.793 ^a	4.988 ^a	5.592	5.998 ^a
0.0		50						86	19	37		35					
0.378		34		51	46	34	60					36				30	27
1.290			62	23	28	44		14	81	43	90	29		37		29	20
2.274		16		26	26						10					19	
2.407			21			22				20			50		60	22	18
2.573			17														
2.671						7									40		
2.686														17			

^aDecays not previously reported.TABLE IV. $^{52}\text{Cr}(p,\gamma)^{53}\text{Mn}$ angular distributions.

Resonance No.	E_i (MeV)	E_f	J_f^π	A_2	A_4	J_i^π	
2	7.925	0.0	$\frac{7}{2}^-$	-0.24(3)	0.16(3)	$\frac{5}{2}^-$	
		1.290	$\frac{3}{2}^-$	0.18(5)	-0.01(5)		
3	7.931	0.0	$\frac{7}{2}^-$	-0.20(3)	0.07(3)	$\frac{5}{2}^-$	
		1.290	$\frac{3}{2}^-$	-0.17(4)	0.12(4)		
		2.407	$\frac{3}{2}^-$	-0.47(7)	0.10(7)		
		3.381	J'	-0.55(6)	0.32(7)	$J' = \frac{3}{2}^-, \frac{7}{2}^-$	
		3.381	0.378	$\frac{5}{2}^-$	0.25(8)		0.28(9)
		7.931	3.709	J'	-0.12(5)		0.01(5)
7	7.978	1.290	$\frac{3}{2}^-$	-0.05(19)	-0.29(21)	$J' = \frac{7}{2}^-$	
		1.441	$\frac{11}{2}^-$	0.13(14)	-0.24(15)		
		1.621	$\frac{9}{2}^-$	-0.67(10)	-0.06(11)		
7	7.978	1.290	$\frac{3}{2}^-$	0.37(11)	-0.09(11)	$\frac{3}{2}^-, \frac{5}{2}^-$	
		2.274	$\frac{5}{2}^-$	-0.30(3)	0.13(3)		
		2.876	$\frac{3}{2}^-$	-0.27(7)	0.17(7)		

TABLE IV. (Continued).

Resonance No.	E_i (MeV)	E_f	J_f^π	A_2	A_4	J_i^π	
9	8.008	0.0	$\frac{7}{2}^-$	-0.28(3)	0.10(4)	$\frac{5}{2}^-$	
		0.378	$\frac{5}{2}^-$	0.29(3)	0.11(3)		
		2.274	$\frac{5}{2}^-$	0.22(3)	-0.03(8)		
		2.686	$\frac{7}{2}^-$	0.09(7)	0.10(8)		
12	8.027	0.0	$\frac{7}{2}^-$	-0.13(3)	0.04(3)	$\frac{5}{2}^-$	
		0.378	$\frac{5}{2}^-$	0.19(14)	0.22(14)		
		2.279	$\frac{5}{2}^-$	0.41(6)	-0.12(6)		
13	8.030	3.097	$\frac{3}{2}^-$	-0.24(6)	0.18(6)	$\frac{3}{2}^-, \frac{5}{2}$	
		3.200	J'	-0.45(5)	0.13(5)		
	3.200	0.0	$\frac{7}{2}^-$	-0.18(7)	0.04(7)	$J' = \frac{5}{2}$	
		0.378	$\frac{5}{2}^-$	0.09(9)	0.18(9)		
		1.290	$\frac{3}{2}^-$	-0.30(6)	-0.05(6)		
	8.030	3.955	J'	-0.37(5)	0.15(5)	$J' = \frac{7}{2}^-$	
		3.955	0.378	$\frac{5}{2}^-$	0.47(15)		0.14(13)
			1.621	$\frac{9}{2}^-$	-0.64(11)	0.05(13)	$J' = \frac{7}{2}^-$
			2.686	$\frac{7}{2}^-$	0.62(4)	-0.44(4)	
			8.030	4.300	J'	-0.33(7)	
	4.300	1.290	$\frac{3}{2}^-$	-0.17(18)	0.17(18)	$J' = \frac{3}{2}^-, \frac{5}{2}$	
14	8.040	2.877	$\frac{3}{2}^-$	-0.11(8)	-0.03(8)	$\frac{3}{2}^-, \frac{5}{2}^-$	
		4.560	J'	-0.13(10)	0.03(10)		
	4.560	1.290	$\frac{3}{2}^-$	-0.05(13)	-0.21(14)	$J' = \frac{1}{2}, \frac{3}{2}^-, \frac{5}{2}$	
		8.040	4.635	J'	-0.35(12)		0.08(13)
	4.635	0.0	$\frac{7}{2}^-$	-0.14(8)	0.20(9)	$J' = \frac{3}{2}^-, \frac{5}{2}^-, \frac{7}{2}^-$	
		1.290	$\frac{3}{2}^-$	0.95(24)	-0.24(27)		
16	8.054	0.0	$\frac{7}{2}^-$	-0.04(6)	0.06(7)	$\frac{5}{2}^-$	
		0.378	$\frac{5}{2}^-$	0.53(7)	0.17(7)		
		2.274	$\frac{5}{2}^-$	0.40(4)	0.04(4)		
		2.407	$\frac{3}{2}^-$	-0.37(4)	0.13(5)		
		2.686	$\frac{7}{2}^-$	0.54(8)	-0.12(9)		
		2.573	$\frac{7}{2}^-$	-0.51(2)	0.30(8)		
		17	8.058	0.0	$\frac{7}{2}^-$		-0.23(7)
0.378	$\frac{5}{2}^-$			0.77(11)	-0.07(19)		
1.290	$\frac{3}{2}^-$			-0.31(4)	0.19(4)		
2.407	$\frac{3}{2}^-$			-0.27(6)	-0.10(6)		
2.274	$\frac{5}{2}^-$			0.35(7)	0.15(6)		
3.129	$\frac{5}{2}^-$			0.38(7)	0.20(7)		
3.595	J'			0.03(12)	0.17(7)	$J' = \frac{3}{2}, \frac{5}{2}, \frac{7}{2}$	

TABLE IV. (Continued).

Resonance No.	E_i (MeV)	E_f	J_f^π	A_2	A_4	J_i^π	
21	8.084	0.378	$\frac{5}{2}^-$	0.36(13)	0.14(14)	$\frac{5}{2}^-$	
		1.290	$\frac{3}{2}^-$	0.40(7)	0.25(7)		
		2.274	$\frac{5}{2}^-$	-0.17(4)	0.12(5)		
		3.097	$\frac{3}{2}^-$	0.10(7)	0.09(7)		
	4.062	0.0	J'	-0.35(10)	0.40(10)	$J' = \frac{3}{2}^-, \frac{5}{2}, \frac{7}{2}^-$	
		8.084	4.552	J'	-0.28(7)		0.14(8)
		4.552	0.0	$\frac{7}{2}^-$	-0.34(9)		0.19(10)
		8.084	5.998	J'	0.21(10)		0.10(10)
22	8.089	0.378	$\frac{5}{2}^-$	0.22(4)	0.13(4)	$\frac{5}{2}^-$	
		2.407	$\frac{3}{2}^-$	-0.30(7)	0.06(8)		
		2.686	$\frac{7}{2}^-$	0.50(6)	-0.14(6)		
23	8.096	0.378	$\frac{5}{2}^-$	0.42(4)	0.25(4)	Doublet: $\frac{3}{2}^-, \frac{5}{2}^-,$ and $\frac{7}{2}^-$	
		1.290	$\frac{3}{2}^-$	-0.35(5)	0.04(5)		
		2.407	$\frac{3}{2}^-$	-0.37(5)	-0.03(5)		
		2.686	$\frac{7}{2}^-$	0.28(4)	0.15(4)		
29	8.136	0.378	$\frac{5}{2}^-$	-0.05(10)	0.18(10)	$\frac{3}{2}^-$	
		1.290	$\frac{3}{2}^-$	0.12(3)	0.17(3)		
		2.407	$\frac{3}{2}^-$	0.36(5)	0.08(5)		
		2.672	$\frac{1}{2}^-$	-0.15(9)	0.05(10)		
	3.182	0.378	$\frac{5}{2}^-$	J'	0.67(12)	0.16(11)	$J' = \frac{3}{2}^-$
		1.290	$\frac{3}{2}^-$	-0.13(5)	0.12(5)		
		1.290	$\frac{3}{2}^-$	-0.04(10)	0.04(11)		
		8.136	4.988	J'	-0.45(14)	0.10(15)	
30	8.141	2.672	$\frac{5}{2}^-$	-0.31(7)	0.10(7)	$\frac{3}{2}^-$	
		2.407	$\frac{3}{2}^-$	0.35(6)	0.10(6)		
		2.672	$\frac{1}{2}^-$	-0.58(3)	0.01(3)		
		2.876	$\frac{3}{2}^-$	0.15(6)	-0.04(1)		
		3.666	$\frac{5}{2}^-$	0.01(5)	0.01(5)		
31	8.159	0.0	$\frac{7}{2}^-$	-0.17(3)	0.15(3)	$\frac{5}{2}, \frac{9}{2}$	
32	8.179	1.290	$\frac{3}{2}^-$	0.27(3)	0.05(3)	$\frac{5}{2}^-$	
		2.407	$\frac{3}{2}^-$	0.42(7)	0.22(7)		
		2.686	$\frac{7}{2}^-$	-0.22(7)	-0.15(8)		
		3.690	J'	0.14(11)	-0.39(11)		
		4.348	J'	-0.05(10)	0.21(8)		

Published γ -decay schemes for the resonances at 1.386, 1.445, 1.497, 1.475, and 1.606 MeV agree qualitatively with the present results although there are a number of differences of detail, probably attributable to different resolutions.^{1,4-8} The remaining eleven resonances were not previously studied.

B. Bound states

Of the 102 bound levels up to 6 MeV in ^{53}Mn at least 13 are of high spin ($\frac{9}{2}$ and above) and not directly accessible in the present study. Of the 47 levels directly populated in this work, only 29 were reported in earlier γ -ray

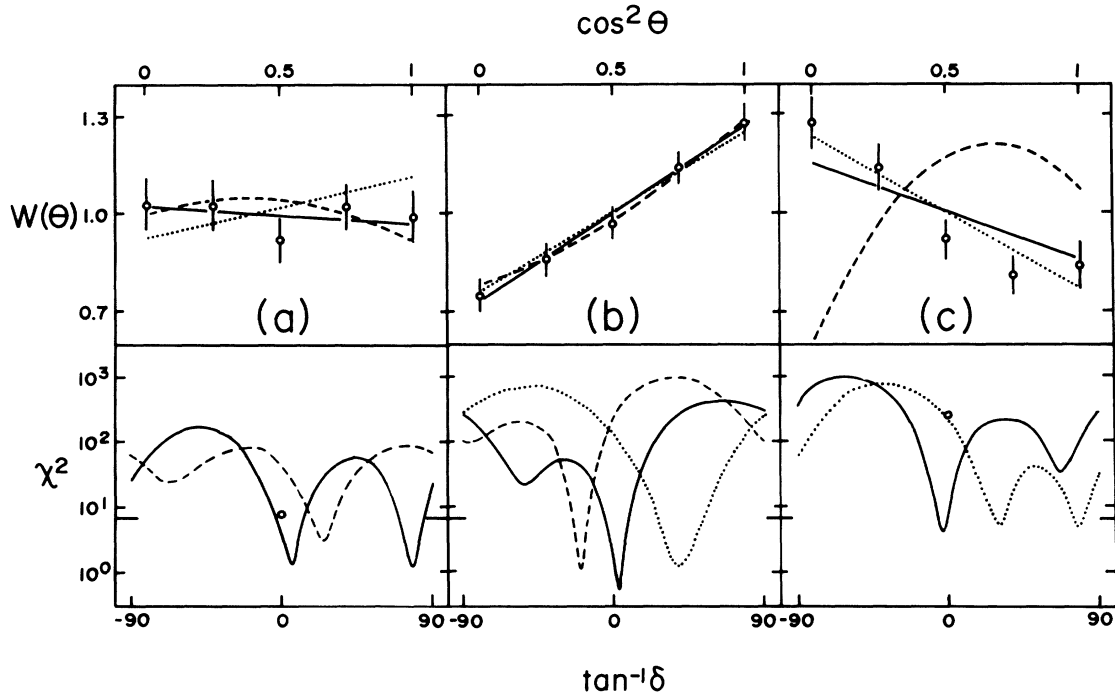


FIG. 4. Angular distribution at Res. No. 16, $E_p = 1.522$ MeV, for primary transitions to (a) $E_x = 0$ ($\frac{7}{2}^-$), (b) $E_x = 2.274$ MeV ($\frac{5}{2}^-$), (c) $E_x = 2.407$ MeV ($\frac{3}{2}^-$), for resonance spins of $\frac{3}{2}$ (dotted), $\frac{5}{2}$ (solid), and $\frac{7}{2}$ (dashed). The 0.1% confidence limit for two degrees of freedom is 6.9. The phase convention for the mixing ratios is that of Rose and Brink (Ref. 10).

studies.¹ In those cases, the agreement is fairly good with the decay schemes indicated in Table III. The other 18 bound states, seen here for the first time in γ decay, have all previously been observed in particle spectroscopy. Of particular note is the high resolution (p, α) study of

Tarara *et al.*⁹ Bound levels at 2.448, 2.761, 2.967, and 2.978 proposed by Schulte *et al.*⁸ were not observed in this work. Reference 9 suggests their placement may be in error.

Although a number of the bound states of unknown

TABLE V. New J^π values for bound states.

E_x (MeV)	(a)	J^π	(b)	E_x (MeV)	(a)	J^π	(b)
3.007	$(\frac{5}{2}^+)$		$(\frac{3}{2}^-, \frac{5}{2}, \frac{7}{2}^-)$	4.266	$(\frac{5}{2}^-, \frac{7}{2}^-)$		$(\frac{3}{2}^-, \frac{5}{2}, \frac{7}{2})$
3.182	$(\frac{3}{2}^-)$		$\frac{3}{2}^-$	4.300	$\frac{5}{2}, \frac{7}{2}^-$		$\frac{3}{2}^-, \frac{5}{2}$
3.200			$\frac{5}{2}$	4.348	$(\frac{1}{2}^-, \frac{3}{2}^-)$		$(\frac{1}{2}^-, \frac{3}{2}, \frac{5}{2}, \frac{7}{2}^-)$
3.381			$\frac{3}{2}^-, \frac{7}{2}^-$	4.362			$(\frac{1}{2}^-, \frac{3}{2}, \frac{5}{2}, \frac{7}{2}^-)$
3.466			$(\frac{3}{2}^-, \frac{5}{2}, \frac{7}{2}^-)$	4.522			$(\frac{1}{2}^-, \frac{3}{2}, \frac{5}{2}, \frac{7}{2}^-)$
3.532			$(\frac{3}{2}^-, \frac{5}{2}, \frac{7}{2}^-)$	4.552			$\frac{5}{2}, \frac{7}{2}^-$
3.595			$\frac{3}{2}^-, \frac{5}{2}, \frac{7}{2}$	4.560			$\frac{3}{2}^-, \frac{5}{2}$
3.709	$(\frac{5}{2}^-, \frac{7}{2}^-)$		$\frac{7}{2}^-$	4.635	$(\frac{5}{2}^-, \frac{7}{2}^-)$		$\frac{3}{2}^-, \frac{5}{2}, \frac{7}{2}^-$
3.955			$\frac{7}{2}^-$	4.762			$(\frac{3}{2}^-, \frac{5}{2}, \frac{7}{2}^-)$
3.960			$(\frac{3}{2}^-, \frac{5}{2}, \frac{7}{2}^-)$	4.780	$(\frac{1}{2}^-, \frac{3}{2}^-)$		$(\frac{1}{2}^-, \frac{3}{2}, \frac{5}{2}, \frac{7}{2}^-)$
3.999			$(\frac{3}{2}^-, \frac{5}{2}, \frac{7}{2}^-)$	4.793			$(\frac{3}{2}^-, \frac{5}{2}, \frac{7}{2}^-)$
4.062	$(\frac{7}{2}^-)$		$\frac{3}{2}^-, \frac{5}{2}, \frac{7}{2}^-$	4.988			$\frac{1}{2}, \frac{3}{2}, \frac{5}{2}^-$
4.083			$(\frac{3}{2}, \frac{5}{2}, \frac{7}{2}^-)$	5.998			$\frac{3}{2}^-, \frac{5}{2}, \frac{7}{2}^-$

^aReference 1.

^bThis work.

TABLE VI. Properties of analog state channels.

E_f (MeV)	$\langle E_x \rangle$ (MeV)	Γ (MeV)	$\Sigma\Gamma_\gamma$ (mW.u.)	J^π_f	C^2S	Notes
0.0	8.027	0.044	60	$\frac{7}{2}^-$	3.0	
0.378	8.029	0.074	100	$\frac{5}{2}^-$	0.1	$(f_{7/2})^5$
1.290	8.053	0.054	55	$\frac{3}{2}^-$	0.2	
2.274	8.053	0.040	160	$\frac{5}{2}^-$		Nonstripping
2.407	8.055	0.011	70	$\frac{3}{2}^-$	1.5	$(f_{7/2})^4 p_{3/2}$
3.129	8.070	0.038	64	$\frac{5}{2}^-$	0.2	
3.666	8.072	0.049	13	$\frac{5}{2}^-$	1.8	$(f_{7/2})^4 f_{5/2}$

spin were strongly populated and both primary and secondary angular distributions were measured, few unambiguous spin assignments were possible, as may be seen in Table V. The previous spins, mostly derived from ($^3\text{He},d$) l values, are consistent with these measurements.

C. The 8.05 MeV $\frac{5}{2}^-$ analog state

Of the 16 resonances whose angular distributions were measured in this work, seven are unambiguously $\frac{5}{2}^-$ states and five others may be. Previous work in proton capture² and proton stripping^{3,4} has identified four $l=3$ levels in the region of the $\frac{5}{2}^-$ analog, at 7.935, 8.000, 8.027, and 8.050 MeV. The final two have been assigned as $\frac{5}{2}^-$ states using ($^3\text{He},dp$) angular correlations.⁴ The resolution possible in the particle work makes positive identification with capture resonances uncertain. However, it seems likely that resonances 2 and 3 may be associated with the first, 9 with the second, 12 to 14 with the third, and 16 and 17 with the fourth particle group. There seems to be no $l=3$ proton stripping corresponding to the $J=\frac{5}{2}$ resonances 21 and 22. The $\frac{3}{2}^-$ resonances 29 and 30 may correspond to the stripping peak at 8.13 MeV.

The eight likely $\frac{5}{2}^-$ levels in the region of the analog state are listed in Table VI. The relative strengths for the different resonances were taken from the yield curve and from the spectra, then normalized to the width for resonance 16 of $(2J+1)\Gamma_\gamma\Gamma_p/\Gamma=0.6$ eV given by Vuister⁵ based on a γ window 4.0–8.5 MeV and having an estimated uncertainty of 50%. From these widths and the branching ratios of Table II, the fragmentation in a number of decay channels leading to final states of large single particle strength was derived. This is shown in Fig. 5, along with the ($^3\text{He},d$) spectroscopic factors.

Because there are few fragments, it is not meaningful to perform a fit of the full skewed Lorentzian (five-parameter) form to the strengths in different capture channels.^{11,12} Figure 5 and Table VI show the results of symmetric (three-parameter) Lorentzian fits. The centroid $\langle E_x \rangle$ and width Γ may be taken as approximations to the position and spreading width of the analog state as seen in different channels. The fragmentation patterns are dissimilar, possibly reflecting the complex nature of the parent state, at 1.006 MeV in ^{53}Cr , which is thought to contain both an $f_{5/2}$ neutron term and one in which a $p_{3/2}$ neutron is coupled to a core excitation, largely of the half-full proton shell, to account for the low energy, reduced stripping strength, and enhanced $E2$ decay to the ground state.^{1,13,14}

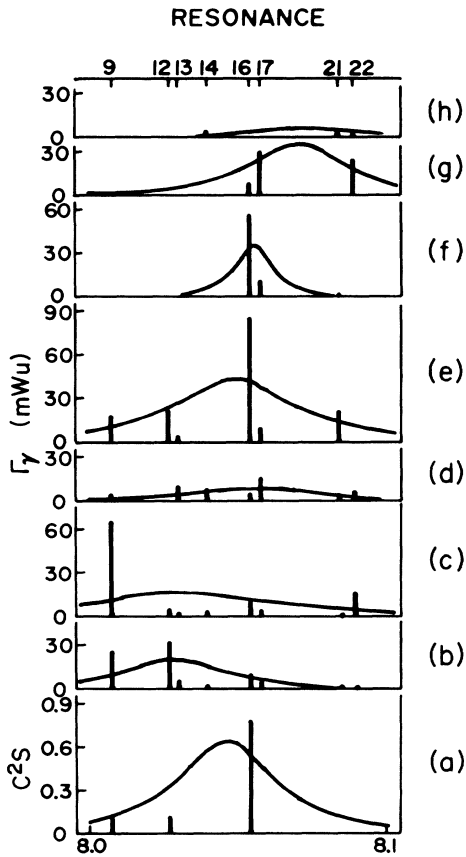


FIG. 5. Fragmentation of the 8.05-MeV $\frac{5}{2}^-$ analog state in (a) ($^3\text{He},d$), and capture to (b) 0.0 ($\frac{7}{2}^-$), (c) 0.378 MeV ($\frac{5}{2}^-$), (d) 1.290 MeV ($\frac{3}{2}^-$), (e) 2.274 MeV ($\frac{5}{2}^-$), (f) 2.407 MeV ($\frac{3}{2}^-$), (g) 3.129 MeV ($\frac{5}{2}^-$), (h) 3.666 MeV ($\frac{5}{2}^-$).

V. CONCLUSIONS

The experiments reported here have demonstrated the existence of up to eight fragments of the analog in ^{53}Mn of the $\frac{5}{2}^-$ 1.006-MeV level of ^{53}Cr . The γ decay of the fragments is consistent with the complex character of the parent state. Almost all the known bound states up to 5 MeV with spins less than $\frac{9}{2}$ were observed, many for the first time in a γ -ray experiment.

ACKNOWLEDGMENTS

The authors are grateful to the operations crews of the King Saud and McMaster accelerators. The experiments were supported by grants from the Research Centre of King Saud University (No. Phys/1409/17) and from the Natural Sciences and Engineering Research Council of Canada.

¹L. K. Peker, Nucl. Data Sheets **43**, 481 (1984).

²G. D. Gunn, J. D. Fox, and G. J. KeKelis, Phys. Rev. C **13**, 595 (1976).

³S. Galès, S. Fortier, H. Laurent, J. M. Maison, and J. P. Schapira, Phys. Rev. C **14**, 842 (1976).

⁴S. E. Arnell, Ark. Fys. **21**, 177 (1962).

⁵P. H. Vuister, Nucl. Phys. **83**, 593 (1966).

⁶S. Maripuu, Nucl. Phys. **A149**, 593 (1970).

⁷R. J. Sparks, Nucl. Phys. **A169**, 113 (1971).

⁸R. L. Schulte, J. D. King, and H. W. Taylor, Nucl. Phys. **A243**,

202 (1975).

⁹R. W. Tarara, J. D. Goss, P. L. Jolivette, G. F. Neal, and C. P. Browne, Phys. Rev. C **13**, 109 (1976).

¹⁰H. J. Rose and D. M. Brink, Rev. Mod. Phys. **39**, 306 (1967).

¹¹J. Sziklai, J. A. Cameron, and I. M. Szöghy, Phys. Rev. C **30**, 490 (1984).

¹²G. U. Din and J. A. Cameron, Phys. Rev. C **35**, 448 (1987).

¹³H. Ohnuma, Nucl. Phys. **88**, 273 (1966).

¹⁴M. Csürös, J. A. Cameron, and Z. Zámori, Can. J. Phys. **49**, 1582 (1971).